

A solver-efficient computational fluid dynamic approach for the thermal performance analysis of ventilated façades

Sofia Pastori^{1*}, Giacomo Scrinzi², Enrico Sergio Mazzucchelli³, and Angelo Lucchini⁴.

^{1*} – Department of Architecture, Built environment and Construction engineering, Politecnico di Milano, Milano (Italy),

sofia.pastori@polimi.it

² – Department of Architecture, Built environment and Construction engineering, Politecnico di Milano, Milano (Italy),

giacomo.scrinzi@polimi.it

³ – Department of Architecture, Built environment and Construction engineering, Politecnico di Milano, Milano (Italy),

enrico.mazzucchelli@polimi.it

⁴ – Department of Architecture, Built environment and Construction engineering, Politecnico di Milano, Milano (Italy),

angelo.lucchini@polimi.it

Abstract

The paper deals with the use of Computational Fluid Dynamics (CFD) for the thermal performance analysis and optimisation of prefabricated Timber-Concrete Composite (TCC) ventilated façades. TCC envelopes are composed of an internal insulated timber-frame wall coupled to an external concrete slab, separated by a ventilated air cavity. Such systems join the properties of engineered timber (good seismic behaviour, low thermal conductivity, environmental sustainability, and ease of system integration) with those of concrete (high thermal inertia, excellent durability and fire resistance). There is very limited knowledge on the performance of TCC façades, especially for what concerns their thermal behaviour. For this reason, a TCC ventilated façade located in the north of Italy was monitored over one year, and the results collected were used to calibrate and validate a CFD model. A new solver algorithm was developed to speed up the CFD simulations, allowing up to 45 times faster analysis compared to conventional solvers. Thanks to this improvement, the final model is suitable to be used for time-efficient thermal analysis (a full-day real-time simulation takes approximately 23 minutes), limiting the expensive and time-consuming construction of mock-ups. The CFD model developed is suitable for the thermal performance analysis and optimisation of TCC ventilated façades, but also for generic ventilated façades with external massive cladding, both in the case of new and existing buildings.

Keywords

Ventilated façade, CFD, Energy efficiency, Timber-concrete composite façade, Building monitoring.

1. Introduction

In recent years, the construction industry has witnessed significant growth in the adoption of engineered timber products, both for new and existing buildings. This is primarily due to their good characteristics, such as excellent seismic performance, good thermal insulation, environmental sustainability and good behaviour under fire. Additionally, timber is highly compatible with prefabrication processes and systems integration, and can be easily disassembled at the end of its lifecycle [1]. On the other side, its limitations are mainly related to its fragile stress-strain behaviour, hygroscopic properties and low durability if not adequately protected [2].

In the realm of building envelopes, lightweight timber façades typically exhibit lower thermal inertia and acoustic insulation than higher-mass alternatives. On the other hand, massive timber solutions involve considerable use of virgin materials and high costs. To address these limitations and enhance performance in terms of structural behaviour, acoustic properties, fire resistance, and durability, timber structures are often combined with concrete, resulting in

50 timber-concrete composite (TCC) systems [3].

51 TCC facades generally consist of an internal insulated timber wall coupled with an external concrete slab, which
52 acts as a protective barrier against adverse weather conditions [4], particularly extreme events like hailstorms and
53 windstorms. These hybrid facades merge the advantages of timber - i.e., light weight, excellent thermal insulation,
54 sustainability, ease of prefabrication and systems integration, aesthetic appeal - with the benefits of concrete - i.e.,
55 mechanical strength, high thermal inertia, good acoustic insulation, durability, fire resistance, application of heavy
56 claddings (e.g., tiles or stone) - [5].

57 Beyond timber-based construction, another widely studied topic is the use of ventilated facades and their advantages
58 in terms of thermal, acoustic, and water-tightness properties [6].

59 TCC technology can be applied to ventilated facades. In this case, the presence of an air cavity between the timber
60 wall and the concrete slab is needed to separate the external (potentially humid) concrete slab and the internal insulated
61 timber wall, which must always be dry to prevent material degradation.

62 A comprehensive evaluation of the thermal performance of ventilated facades remains a key focus in current
63 research. These systems interact in complex ways with the external environment, necessitating experimental
64 investigations and CFD analyses to model the airflow within the cavity [7]. Over the past two decades, numerous studies
65 explored the thermal behaviour of ventilated facades through experimental and numerical approaches [7,8]. Typically,
66 these studies involve experimental monitoring, followed by analytical or CFD-based assessments. However, only a
67 limited number of these CFD studies validate their findings against experimental data. Experimental monitoring,
68 barring unexpected sensor errors, tends to yield reliable results, but these are closely tied to specific case studies [9].
69 On one hand, analytical methods have a long-established history and are known for their reliability, as evidenced by
70 numerous studies. These methods involve simplified processes grounded in physical correlations, whose validity has
71 been repeatedly confirmed over time [10]. On the other hand, CFD simulations provide a higher degree of detail, but
72 are relatively new and less extensively validated, leading to greater uncertainties and the need for experimental
73 validation [4]. One of the primary challenges in applying CFD techniques within the building physics domain is the
74 significant computational power required [11]. This limitation has historically confined CFD studies to steady-state
75 analyses or very short dynamic periods [12-14]. Despite these challenges, CFD's ability to deliver highly precise
76 information about flow fields makes it a valuable tool for evaluating the impact of design details in ventilated facades.
77 For instance, research has examined airflow around window blinds [15], facade openings [16], and various shading
78 systems [17].

79 The integration of experimental analysis and CFD modelling is widely regarded as the most comprehensive and
80 accurate approach to evaluating the thermal behaviour of ventilated facades [9]. This combination was considered for
81 the current investigation of ventilated facades with external massive cladding. Specifically, a TCC envelope was
82 examined, a topic with limited prior research [18], and for which no rigorous CFD modelling studies have been
83 identified.

84 The objective of the research was to develop a solver-efficient CFD model for analysing the thermal performance of
85 ventilated façades. Specifically, the first sub-goal was to implement the model and a novel solver algorithm to speed
86 up the simulation process compared to conventional solvers. The second sub-goal was the model calibration and
87 validation against experimental results, which were previously collected during the façade monitoring over one entire
88 year [19].

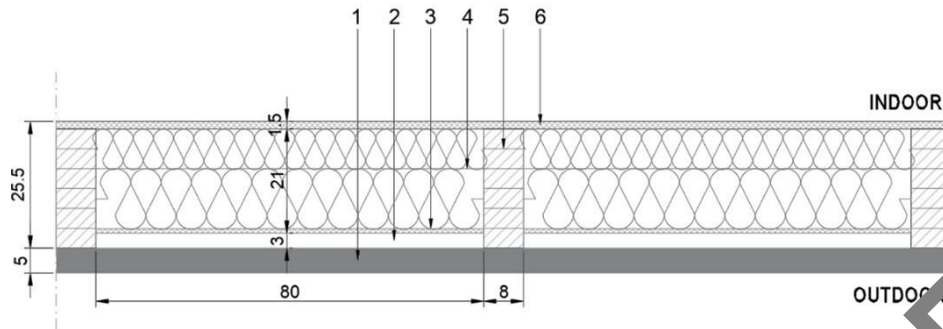
89 The innovative aspect of the research is the implementation of a fast and accurate CFD model for the thermal
90 performance prediction and optimization of ventilated facades with massive cladding, which can be used for new or
91 refurbished buildings.

92 2. Methods

93 For the development of the CFD model, the prefabricated TCC ventilated façade system in Fig. 1 was considered. It
94 is composed of an internal timber frame structure coupled with an external 50 mm thick reinforced concrete slab,
95 separated by independent vertical ventilated air cavities. The concrete slab has sealed joints, which means that each air
96 cavity is connected to the external environment only at the bottom and top of the façade. The height of the air cavity
97 depends on the building elevation and the presence of windows and/or protruding slabs.

98 The thermal behaviour of the TCC façade was preliminary monitored experimentally, to collect all the data needed
99 for calibrating the numerical model. For this purpose, a 3-storey building with a TCC ventilated envelope was built and
100 monitored for over a year in the north of Italy. In this case, the ventilated façade's height is equal to two storeys of the
101 building (the ground floor has a different envelope system), which is the minimum height that allows us to gain some
102 benefits from the natural ventilation inside the cavity of the façade, according to the literature. The monitoring started
103 in August 2022 and ended in August 2023 [19]. The collected data were then used to set, calibrate and validate the CFD

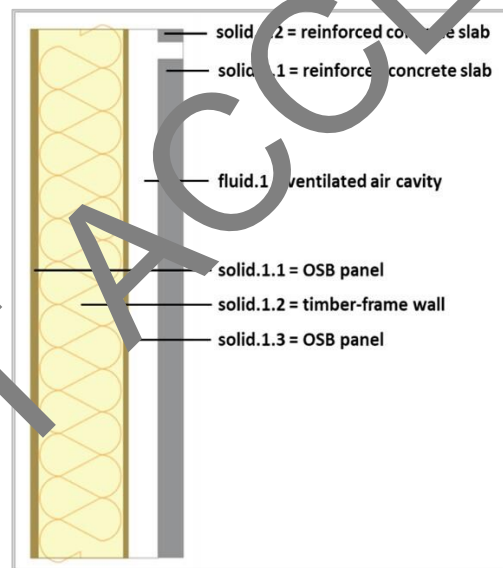
104 model, which was developed using the open-source software OpenFOAM [20]. All simulations were run on a computer
105 with Dual XEON 6x CPUs and 48 GB of RAM.
106



107
108 Figure 1 – Horizontal section of the TCC façade studied (units in cm). The layers are: (1) reinforced concrete slab, (2)
109 ventilated air cavity, (3) OSB panel, (4) rockwool insulation (100 kg/m³), (5) timber-frame structure and (6) OSB panel.
110 © Pastori S.

111 2.1 Geometry of the model

112 A two-dimensional analysis was performed to keep the model as simple as possible. This choice was compatible
113 with the envelope configuration, since the air flows through many vertical independent façade cavities characterized
114 by limited width (800 mm), hence horizontal air flow is negligible. For this reason, a 2D model that neglects the third
115 spatial dimension was considered adequate for the study purpose. The model geometry developed is shown in Fig. 2.
116



117
118 Figure 2 – Two-dimensional CFD model developed with indication of the solid and fluid regions. © Pastori S.

119 2.2 Physical properties of the model

120 The thermo-physical properties assigned to each material (i.e. each region) in the CFD model are reported in **Errore.**
121 **L'origine riferimento non è stata trovata.** The materials' characteristics were taken from the technical datasheets of
122 the products used for the envelope.
123

Table 1 – Physical properties of the regions of the CFD model.

Solid regions						
Region	Density (kg/m ³)	Thermal conductivity (W/mK)	Specific heat at constant pressure (J/kgK)	Emissivity	Absorptivity	
Solid.1.1 = Internal OSB panel	550	0.100	1600	0.8	0.8	
Solid.1.2 = Timber-frame insulated wall	100	0.035	1030	0.8	0.8	
Solid.1.3 = External OSB panel	600	0.100	1600	0.8	0.8	
Solid.2.1/2.2 = Concrete slab	2400	2.00	1000	0.5	0.5	
Fluid region						
Region	Density (kg/m ³)	Thermal conductivity (W/mK)	Specific heat at constant pressure (J/kgK)	Dynamic viscosity (Pa·s)	Molar mass (kg/kmol)	Prandtl number
Air (properties at 30°C)	Variable, function of temperature (incompressible ideal gas)	0.02588	1007	1.872 · 10 ⁻⁵	28.966	0.728

124 **2.3 Boundary conditions**

125 The boundary conditions applied to the model are shown in Figure 3 – . The trends of the variables $T_{air,i}$ (indoor
 126 air temperature), $T_{air,e}$ (outdoor air temperature), $q_{r,incident}$ (incident solar irradiation on the facade), and $V_{air,e}$
 127 (air velocity at the bottom inlet of the cavity) were taken from the experimental monitoring. The values of h_i
 128 (convective-radiative coefficient of indoor environment), h_e (convective-radiative coefficient of outdoor environment),
 129 R_{se} (surface resistance of outdoor environment) were taken from the Standard ISO 6946 [21]; the values of T_{outlet}
 130 (air temperature at the top outlet of the cavity), P_{outlet} (air pressure at the top outlet of the cavity), V_{outlet} (air
 131 velocity at the top outlet of the cavity) are calculated by the software during the simulation.
 132

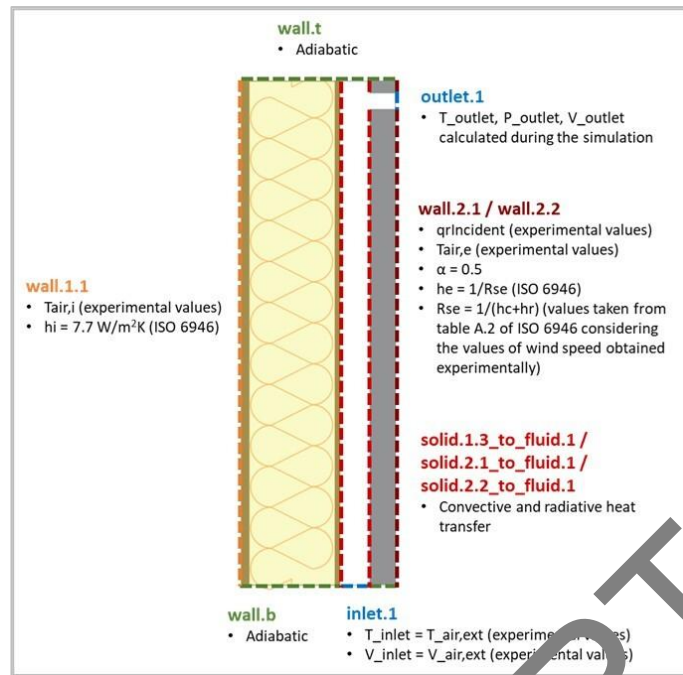


Figure 3 – Main boundary conditions applied to the CFD model. © Pastori S.

2.4 Mesh

A mesh refinement study was developed to identify the best model discretization in terms of accuracy of the results and computational cost/time. Three meshes were tested by setting a simple simulation case, and the accuracy of the results obtained from the simulations was compared.

The meshes tested were:

- m0001_baseMesh
- m0002_baseMeshx1.5
- m0003_baseMeshx1.5x1.5

The number of cells for each mesh is equal to the number of the previous one multiplied by 1.5 in both vertical and horizontal directions. As expected, the results obtained show that the grid refinement produces slightly better accuracy, but with higher computational time. In this specific case, the mesh refinement does not produce consistent differences in the results, while the time needed for the computation increases considerably (see **Errore. L'origine riferimento non è stata trovata.**). For this reason, the coarser mesh (m0001) was chosen and used for all the simulations (Fig. 4).

The first simulation (t0001) was run for 96 hours (4 days) to evaluate the amount of time needed by the model to catch the correct temperature trends. According to the results, 48 hours were enough for that, thus the second case (t0002) was run for 48 hours. The third simulation (t0003) was stopped just after 24 hours due to the huge computational time required to end the analysis.

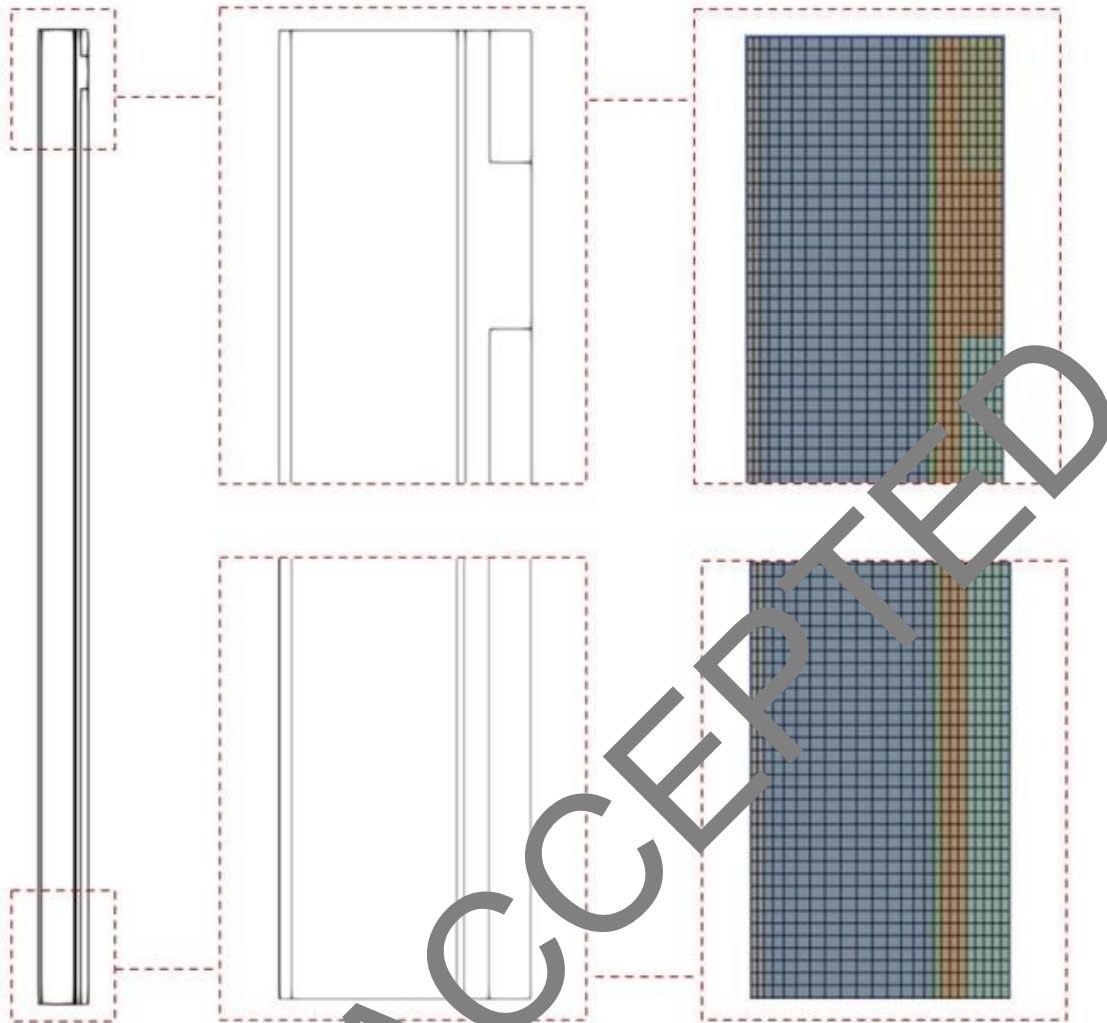


Figure 4 – CFD model geometry and mesh. © Pastori S.

Table 2 – Mesh refinement study.

Mesh refinement					
Simulation	Mesh	Solver	Time simulated	Time needed for running simulation	Temperatures that differ more than 0.2K from t0001
t0001	m0001 (7112 cells)	chtMultiRegionFoam	96h (345000 s)	67.5h	/
t0002	m0002 (14850 cells)	chtMultiRegionFoam	48h (172800 s)	100h (+196% t0001)	1.4%
t0003	m0003 (33075 cells)	chtMultiRegionFoam	24h (86400 s)	314h (+1761% t0001)	5.7%

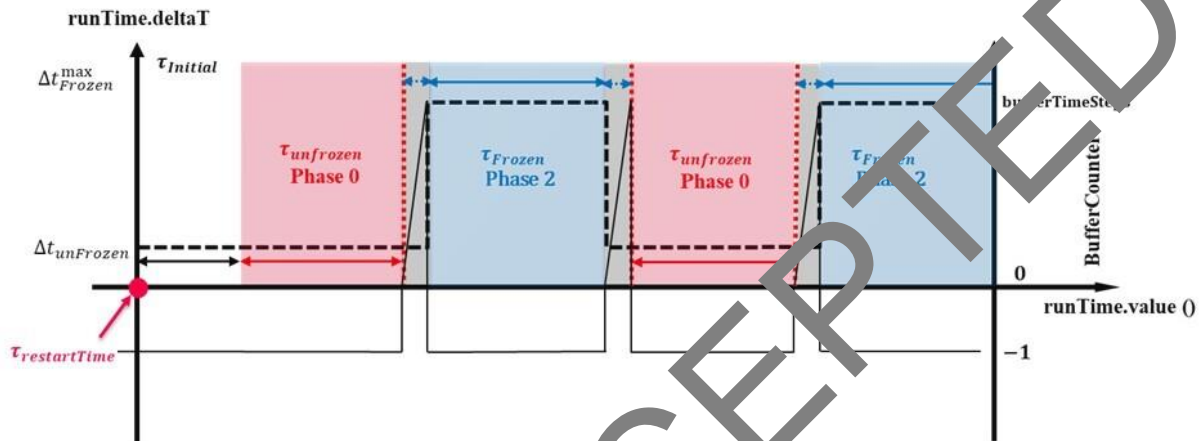
153
 154

155 *2.5 The new "frozen-unfrozen flow" solver*

156 At first, the conventional solver "chtMultiRegionFoam" was used. This solver allows for coupling a transient fluid
 157 flow with heat transfer between regions, buoyancy effects, turbulence, and radiation. It follows a segregated solution
 158 strategy, which means that the equations for each variable characterizing the system are solved sequentially and the
 159 solution of the preceding equations is inserted into the subsequent equation. The coupling between fluid and solid
 160 regions follows the same strategy: first, the equations for the fluid are solved using the temperature of the solid of the
 161 preceding iteration to define the boundary conditions for the temperature in the fluid. After that, the equation for the
 162 solid is solved using the temperature of the fluid of the preceding iteration to define the boundary condition for the

163 solid temperature. This iterative procedure is executed until convergence is achieved. For each fluid region, the
 164 compressible Navier-Stokes equations are solved; for the solid regions, only the energy equation has to be solved. The
 165 regions are coupled by a thermal boundary condition.

166 Starting from that, a novel solver algorithm called the "frozen-unfrozen flow" was developed to speed up the
 167 simulations, by switching the solution mode to "frozen" (i.e. no update of the velocity and pressure fields, allowing
 168 large time steps) and "unfrozen" (i.e. solution of all transport equations, with normal time steps) sequentially. The
 169 normal time step in the "unfrozen" mode is determined by the Courant number and the solid diffusion numbers, while
 170 the time stepping in the "frozen" mode is set based on user input. Fig. 5 shows the schematic view of this algorithm: it
 171 starts with the initial time ($\tau_{initial}$) and several cycles with unfrozen (red zones) and frozen (blue zones) mode are
 172 repeated till the end of the simulation. For stability reasons, a transition mode (grey zones) is considered when the flow
 173 mode is switched between "frozen" and "unfrozen".
 174



175
 176 Figure 5 – Schematic view of the new "frozen-unfrozen flow" solver algorithm. © Pastori S.

177 **2.6 Testing of the new solver**

178 New cases were created to test the new solver performance, varying the length of frozen and unfrozen periods of
 179 time, respectively τ_{frozen} and $\tau_{unfrozen}$, in a systematic way to explore the effect of these numerical parameters on the
 180 accuracy of the results (i.e. the temperature values obtained in the model) and the time needed for the computation. The
 181 new cases were compared to a baseline case t0001, identical to the new ones but run with the old solver. **Errore.**
 182 **L'origine riferimento non è stata trovata.** resumes the results obtained from the new cases. All the simulations were
 183 run for 24 hours real time.

184 As expected, the simulation speed increased by increasing the ratio $\tau_{frozen} / \tau_{unfrozen}$, while the accuracy did not appear
 185 to be inversely proportional to the speed.
 186

Table 3 – Cases run for testing the new solver and finding the optimal settings considering the trade-off between speed and result accuracy.

Case	tauFrozen/ tauUnfrozen	Simulation speedup compared to t0001	Max temperature difference (°C) from t0001	% of values that differ more than 0.2°C from t0001	% of values that differ more than 0.5°C from t0001	% of values that differ more than 1°C from t0001
t0011	5s/5s = 1	x 1.8	-2.61 (outlet.1)	12.9%	7.6%	3.9%
t0012	10s/5s = 2	x 2.7	3.61 (outlet.1)	15.5%	8.0%	4.1%
t0013	15s/5s = 3	x 3.5	-2.87 (outlet.1)	16.6%	7.7%	4.3%
t0014	50s/5s = 10	x 9.4	3.20 (outlet.1)	12.4%	2.8%	1.0%
t0015	100s/5s = 20	x 16.5	2.66 (outlet.1)	12.6%	2.9%	1.3%
t0016	500s/5s = 100	x 45	3.43 (outlet.1)	20.8%	9.9%	4.1%

187 2.7 CFD model calibration

188 The calibration process was developed by comparing the results obtained from the CFD model with the experimental
189 data collected. It consisted of changing the physical and numerical parameters used in the modelling until the CFD
190 results were aligned with the experimental ones.

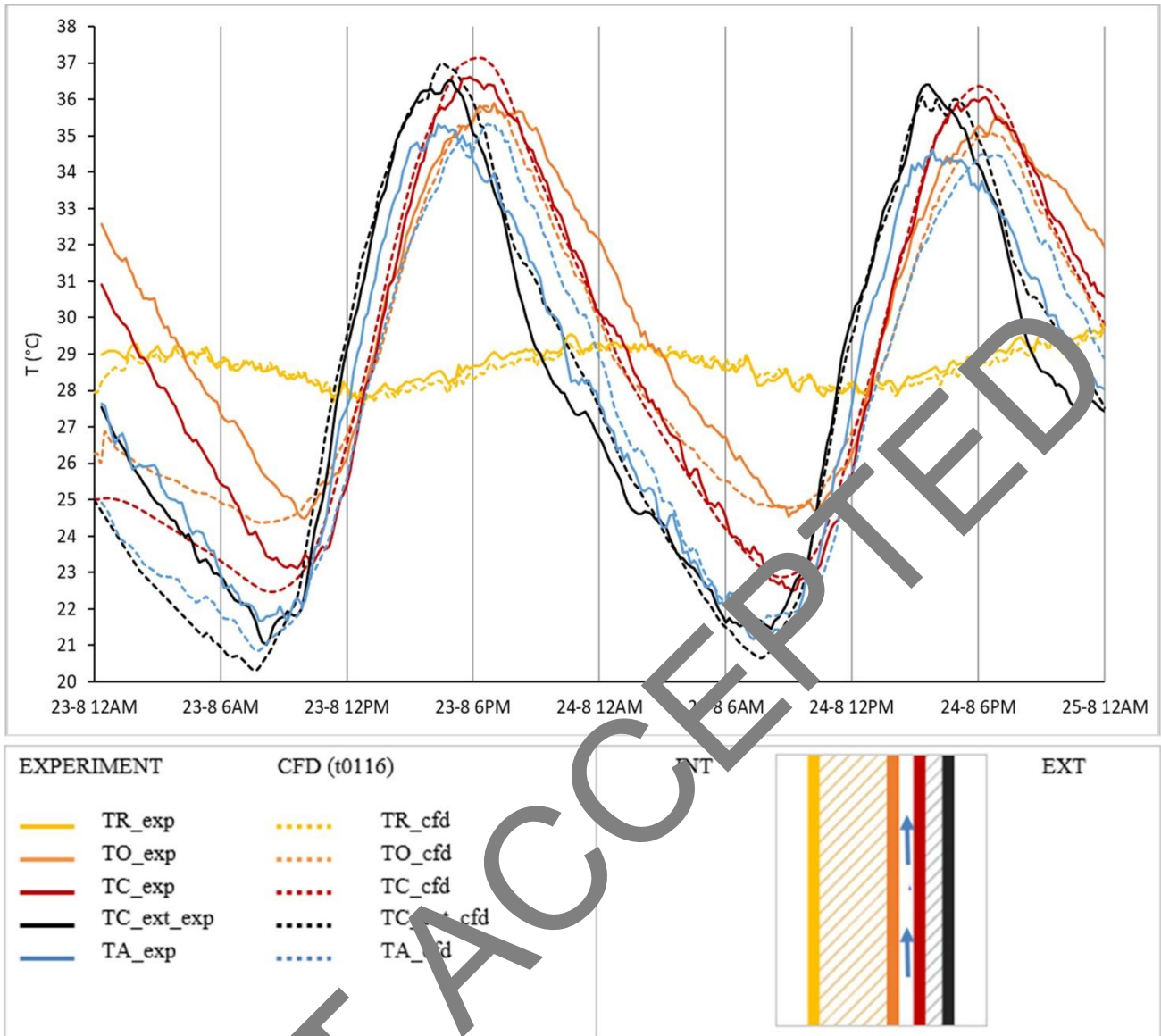
191 For this process, the experimental data collected during summer days with clear sky (from the 23rd to the 27th of
192 August 2022) for the south-oriented building façade were considered. The solver chtMultiRegionFoam was used for
193 the calibration process, since the "frozen-unfrozen flow" solver was still under development.

194 2.8 CFD model validation

195 After calibrating the CFD model against experimental results obtained during summer days with a clear sky, the
196 model was tested again considering different weather conditions. This process serves as model validation and is
197 necessary to see whether the developed model also works under different boundary conditions. In this case, the
198 experimental data collected during summer days with an overcast sky (registered from the 17th to the 21st of August
199 2022) were considered. The façade considered was again the south elevation of the building. For the present research
200 objective, the validation process to test the model accuracy was performed considering only one new case. A more in-
201 depth study should involve a greater number of cases for model validation, testing the calibrated model by changing
202 several parameters (e.g. cavity depth, different weather conditions, etc.).

203 3. Results

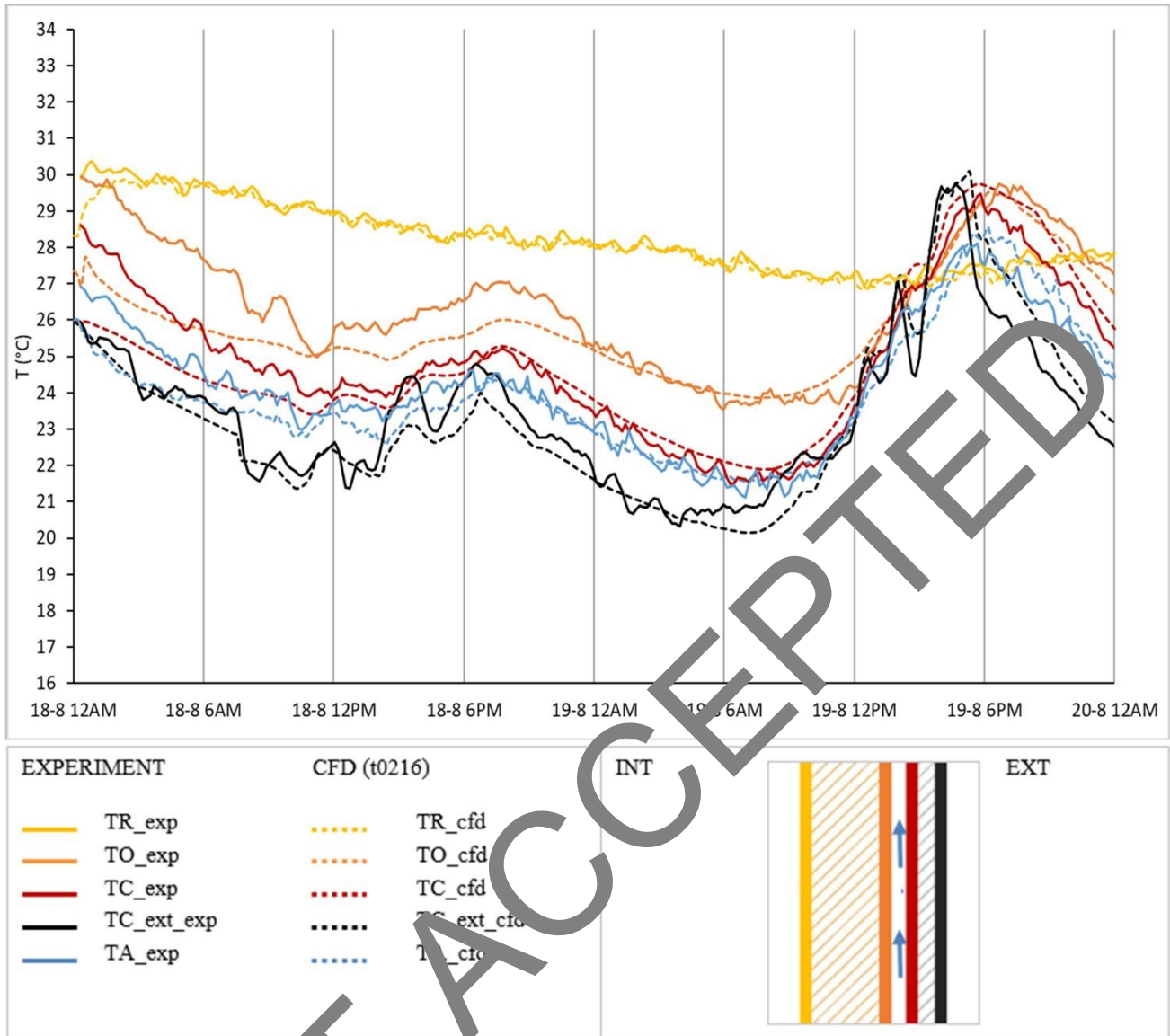
204 In this chapter, the results obtained by running the CFD model developed are presented and discussed. Fig. 6 shows
205 the graphical comparison between the temperatures measured experimentally and those predicted by the calibrated CFD
206 model. The calibrated model (t0116) was able to predict the façade thermal behaviour with a very limited error
207 compared to the experimental values obtained. The error was calculated for each surface of the wall as the difference
208 between the mean temperature measured experimentally on that surface and the one calculated on the same surface by
209 using the CFD model. For the error calculation, only the last 24 hours of each simulation were considered to exclude
210 inaccurate values due to the initialization process at the beginning of each CFD case. The error obtained between
211 experiment and CFD is: 0.19°C for TR, 1.3°C for TO, 0.8°C for TC and 0.9°C for TC_ext. Thus, the mean error between
212 the values measured experimentally and those obtained from the CFD model is 0.8°C.
213



214
 215 Figure 6 – Comparison between the temperatures from the experimental monitoring and those given by the CFD model,
 216 considering a façade facing south and summer days with clear sky. © Pastori S.

217 *3.1 Validated model*

218 The calibrated model (t0116) was then tested considering different boundary conditions, in order to evaluate the
 219 accuracy of the prediction, also for a different case. For this reason, a new case (t0216) was set up by changing the
 220 weather conditions to summer days with an overcast sky. Fig. 7 shows the comparison between the CFD results and
 221 the experimental data. In this case, the error obtained between experiment and CFD is: 0.22°C for TR, 0.8°C for TO,
 222 0.6°C for TC and 0.6°C for TC_ext. Thus, the mean error between the values measured experimentally and those
 223 obtained from the CFD model is 0.6°C, slightly lower than the previous case.
 224



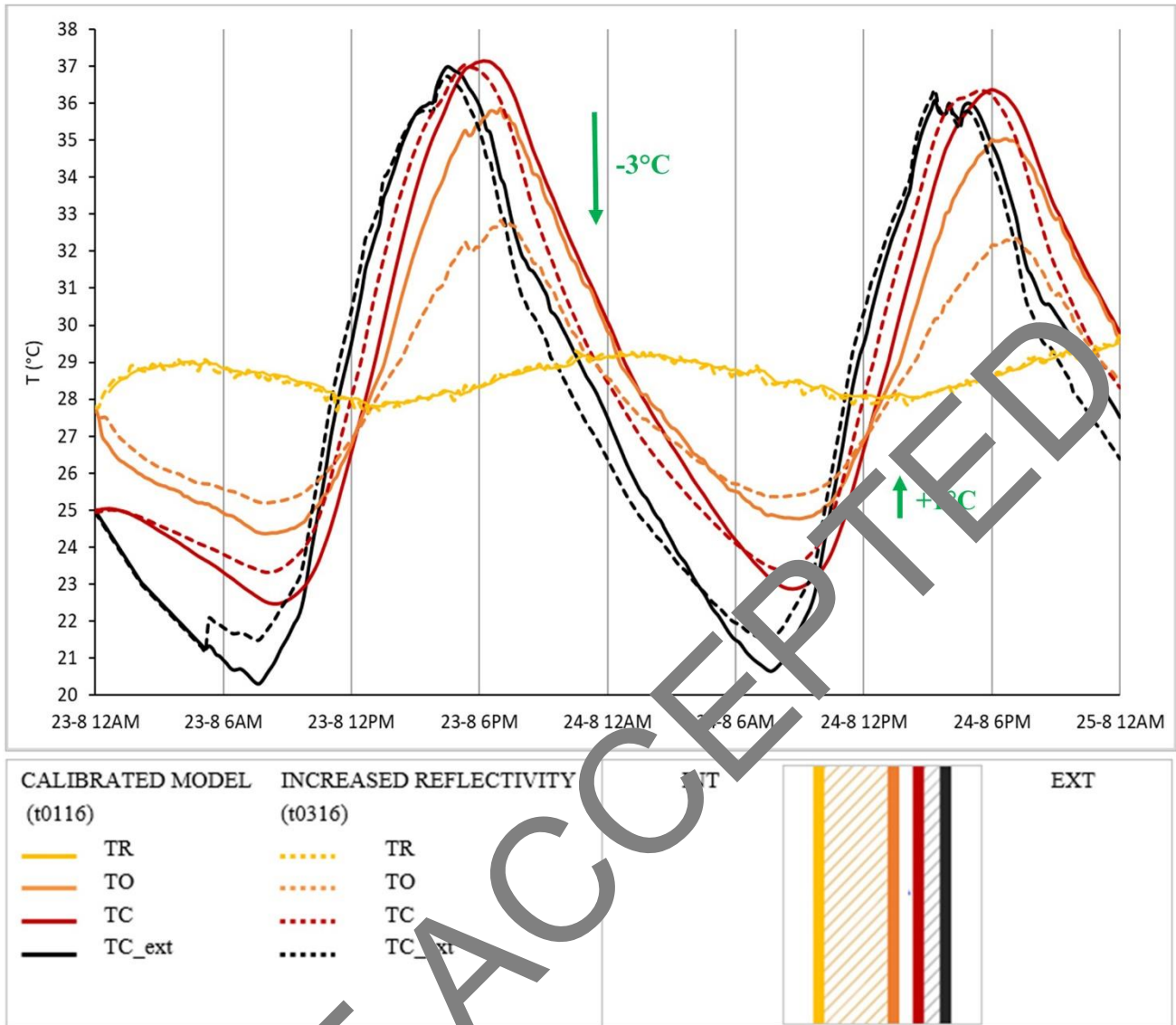
225
 226 Figure 7 – Comparison between the temperatures from the experimental monitoring and those given by the CFD model,
 227 considering a façade facing south and summer days with overcast sky. © Pastori S.

228 *3.2 Prediction of the thermal behaviour*

229 After the CFD model validation, some of the input parameters might be changed (e.g. façade geometry, materials,
 230 weather conditions, etc.) to understand their influence on the facade's thermal behaviour and study an optimised
 231 envelope configuration.

232 For example, the emissivity of the OSB panel facing the ventilated cavity was changed, and the results were analysed.
 233 The objective was to evaluate and quantify the effect of an increased reflectivity of the inner surface of the ventilated
 234 cavity – that can be obtained by painting the OSB panel with a reflective paint or by placing a reflective foil on it – on
 235 the envelope's thermal behaviour, considering summer days with a clear sky.

236 The comparison between the calibrated model (t0116) and the new case with increased reflectivity (t0316) is shown
 237 in Figure 8 – 8. What can be noticed is that an increase from 0.2 to 0.8 in the reflectivity value can produce a 3°C
 238 reduction of TO maximum peaks and a 1°C increase of the lowest peaks. The results show a change in the heat flux
 239 entering the building from 10 W/m² to -10 W/m² over the day.
 240



241
 242 Figure 8 – Comparison between the temperatures predicted by case t0116 (calibrated CFD model) and t0316 (case with
 243 increased reflectivity of the OSB panel into the ventilated cavity). © Pastori S.

244 **4. Conclusions**

245 The research presented focuses on the development of a solver-efficient multi-region 2D CFD model for the thermal
 246 analysis and optimisation of ventilated facades with external massive cladding. The CFD model was calibrated and
 247 validated against the data collected during the experimental monitoring of the timber-concrete composite ventilated
 248 façade of a new building located in the north of Italy (described in [19]). Several CFD models for the thermal analysis
 249 of ventilated facades were found in the literature, however they were all tested to study ventilated facades with thin
 250 external cladding. In contrast, the current research focused on the development of a CFD model for ventilated facades
 251 with external massive cladding.

252 The model was set by using the open-source software OpenFOAM [20] to make it accessible to everyone. Also, it
 253 was developed in two dimensions to be as simple as possible and it was enhanced in terms of computational effort: a
 254 mesh refinement study was performed to select the optimal discretization. Finally, a new "frozen–unfrozen flow" solver
 255 was implemented to allow faster simulations while still maintaining good accuracy of the results. In case the "frozen–
 256 unfrozen flow" solver is used, the simulations are much faster than using the original solver: considering simulations
 257 for 24 h real-time, the new solver can increase the speed of the simulation up to 45 times, keeping an acceptable margin
 258 of error in the results. This significant acceleration is impressive when considering the relatively simple modification
 259 of the algorithm.

260 The calibrated CFD model obtained can be used to assess the thermal performance of TCC ventilated facades in

261 different configurations (e.g., a different air cavity depth, concrete slab thickness, colour and material of the surfaces,
262 orientation, ventilation type, etc.), allowing the optimization of the building envelope solutions, partially avoiding the
263 expensive and time-consuming construction of mock-ups. Accurate research in this respect might be interesting for
264 system manufacturers, in order to further develop their products to comply with the different project requirements, and
265 for designers, to better choose and specify the systems to be used. Certainly, experiments for validation remain key for
266 benchmarking a CFD model prediction. However, the new opportunities offered by calibrated CFD models for facades
267 more than balance the efforts needed to create them from our perspective.

268 Additionally, the study represents an important step towards digital twins for TCC ventilated facades, since the
269 calibrated CFD model can make predictions faster than real-time [22]. For example, the model might be used together
270 with advanced control strategies to minimize a building's energy consumption. A 1:1 digital twin of the façade is
271 required, which might necessitate the digitalization of existing buildings. Future work might address these limitations,
272 e.g., through a refined validation study or a sensitivity analysis with respect to the assumed boundary conditions to
273 mitigate these limitations.

274 At a broader level, the research aims to contribute to the knowledge regarding the thermal performance of ventilated
275 facades composed of an internal lightweight wall structure and an external massive cladding.

276 5. Authors Contributions

277 Conceptualization, P.S.; Methodology, P.S.; Software, P.S.; Validation, P.S.; Formal Analysis, P.S.; Investigation, P.S.;
278 Data Curation, P.S.; Writing – Original Draft Preparation, P.S.; Writing – Review & Editing, P.S. and S.G.;
279 Visualization, P.S. and S.G.; Supervision, M.E.S. and L.A.; Project Administration, M.E.S. and L.A.

280 6. References

- 281 [1] Asdrubali F, Ferracuti B, Lombardi L et al (2017) A Review of Structural, Thermo-Physical, Acoustical, and
282 Environmental Properties of Wooden Materials for Building Applications. *Building and Environment* 114:307–
283 332.
- 284 [2] Janssen H (2018) Characterization of Hygrothermal Properties of Wood-Based Products—Impact of Moisture
285 Content and Temperature. *Constr. Build. Mater* 185: 9–43.
- 286 [3] Fortuna S, Mora TD, Peron F, Magnoni P (2017) Environmental Performances of a Timber-Concrete
287 Prefabricated Composite Wall System. *Energy Procedia* 113:90–97.
- 288 [4] Pastori S, Mereu R, Mazzacchelli ES et al (2021) Energy Performance Evaluation of a Ventilated Façade System
289 through Cfd Modeling and Comparison with International Standards. *Energies* 14:193. doi:10.3390/en14010193.
- 290 [5] Destro R, Bosetto G, Mazzali U et al (2015) Structural and Thermal Behaviour of a Timber-Concrete
291 Prefabricated Composite Wall System. *Energy Procedia* 78:2730–2735.
- 292 [6] Patania R, Gagliano A, Nocera F et al (2010) Thermofluid-Dynamic Analysis of Ventilated Facades. *Energy*
293 *Build.* 42:1108–1117. doi:10.1016/j.enbuild.2010.02.006.
- 294 [7] Giancola E, San Juan C, Blanco E, Heras MR (2012) Experimental Assessment and Modelling of the Performance
295 of an Open Joint Ventilated Façade during Actual Operating Conditions in Mediterranean Climate. *Energy Build.*
296 54:360–375. doi:10.1016/j.enbuild.2012.07.035.
- 297 [8] Ciampi M, Leccese F, Tuoni G (2003) Ventilated Facades Energy Performance in Summer Cooling of Buildings.
298 *Sol. Energy* 75:491–502. doi:10.1016/j.solener.2003.09.010.
- 299 [9] Giancola E, Sánchez MN, Friedrich M et al (2018) Possibilities and Challenges of Different Experimental
300 Techniques for Airflow Characterisation in the Air Cavities of Façades. *J. Facade Des. Eng.* 6:34–48.
301 doi:10.7480/jfde.2018.3.2470.
- 302 [10] Gagliano A, Nocera F, Aneli S (2016) Thermodynamic Analysis of Ventilated Façades under Different Wind
303 Conditions in Summer Period. *Energy Build.* 122:131–139. doi:10.1016/j.enbuild.2016.04.035.
- 304 [11] Jensen J, Bartak M, Drkal F (2007) Modeling and Simulation of a Double-Skin Facade System. In ASHRAE

- 305 Transactions; Symposia, HI-02-21-3.
- 306 [12] Manz H (2003) Numerical Simulation of Heat Transfer by Natural Convection in Cavities of Façade Elements. *Energy Build.* 35:305–311. doi:10.1016/S0378-7788(02)00088-9.
- 307
- 308 [13] Xamán J, Álvarez G, Lira L, Estrada C (2005) Numerical Study of Heat Transfer by Laminar and Turbulent
309 Natural Convection in Tall Cavities of Façade Elements. *Energy Build.* 37:787–794.
310 doi:10.1016/j.enbuild.2004.11.001.
- 311 [14] Pappas A, Zhai Z (2008) Numerical Investigation on Thermal Performance and Correlations of Double Skin
312 Façade with Buoyancy-Driven Airflow. *Energy Build.* 40:466–475. doi:10.1016/j.enbuild.2007.04.002.
- 313 [15] Safer N, Woloszyn M, Roux JJ (2005) Three-Dimensional Simulation with a CFD Tool of the Airflow Phenomena
314 in Single Floor Double-Skin Façade Equipped with a Venetian Blind. *Sol. Energy* 79:193–207.
- 315 [16] Sanjuan C, Suárez MJ, González M et al (2011) Energy Performance of an Open-Join Ventilated Façade
316 Compared with a Conventional Sealed Cavity Façade. *Sol. Energy* 85:1851–1863.
317 doi:10.1016/j.solener.2011.04.028.
- 318 [17] Baldinelli G (2009) Double Skin Façades for Warm Climate Regions: Analysis of a Solution with an Integrated
319 Movable Shading System. *Build. Environ.* 44:1107–1118. doi:10.1016/j.buildenv.2009.08.005.
- 320 [18] Stazi F, Ulpiani G, Pergolini M et al (2018) Experimental Comparison between Three Types of Opaque Ventilated
321 Façades. *Open Constr. Build. Technol. J.* 12:296–308. doi:10.1174/1874-36801812010296.
- 322 [19] Pastori S (2024) Timber-Concrete Composite Ventilated Envelope Systems. Experimental and Numerical
323 Investigations for Thermal Performance Control and Optimization. Ph.D. Thesis, Politecnico di Milano, Milan,
324 Italy, 2024.
- 325 [20] OpenFOAM® v2206. <https://www.openfoam.com/>. Accessed 28 Oct 2025
- 326 [21] EN ISO 6946:2017 Components and Building Elements—Thermal Resistance and Thermal Transmittance—
327 Calculation Methods.
- 328 [22] Tahmasebinia F, Lin L, Wu S et al (2025) Exploring the Benefits and Limitations of Digital Twin Technology in
329 Building Energy. *Appl. Sci.* 13:8814.